Adsorption of Adhesive Proteins from the Marine Mussel, *Mytilus edulis*, on Polymer Films in the Hydrated State Using Angle Dependent X-ray Photoelectron Spectroscopy and Atomic Force Microscopy

Ace M. Baty,[†,‡] Pam K. Leavitt,[⊥] Christopher A. Siedlecki,[∥] Bonnie J. Tyler,[†,‡] Peter A. Suci,[†] Roger E. Marchant,[∥] and Gill G. Geesey*[,†,§]

Center for Biofilm Engineering, 366 EPS Building, P.O. Box 173980, Montana State University, Bozeman, Montana 59717, Department of Chemical Engineering, 306 Cobleigh Hall, Montana State University, Bozeman, Montana 59717, Department of Microbiology, 109 Lewis Hall, Montana State University, Bozeman, Montana 59717, Department of Biomedical Engineering, Case Western Reserve University, Cleveland, Ohio 44106, and Physical Electronics Inc., Eden Prairie, Minnesota 55344

Received November 5, 1996. In Final Form: July 23, 1997[⊗]

The adsorption of mussel adhesive protein (MAP) from the marine mussel *Mytilus edulis* has been investigated on polystyrene (PS) and poly(octadecyl methacrylate) (POMA) surfaces using angle dependent X-ray photoelectron spectroscopy (XPS) and atomic force microscopy (AFM). AFM images previously published in the dehydrated state using contact mode are compared with images acquired in the hydrated state using fluid Tapping Mode to assess the contribution that hydration has on the architecture of the adsorbed proteins. To further characterize the adsorbed protein layer, XPS analysis was performed at liquid nitrogen (LN_2) temperature without dehydrating the samples and at room temperature after the surfaces were dehydrated. The differences observed upon dehydration can be attributed to the strength of the interactions between MAP and the two surfaces. The AFM and XPS data indicate that adsorbed MAP is stabilized on the surface of the PS through interactions that prevent the protein layer from being disrupted upon dehydration. The adsorbed MAP on the POMA surface is representative of a loosely bound protein layer that becomes highly perturbed upon dehydration.

Introduction

The marine mussel, *Mytilus edulis*, produces a series of adhesive proteins that allow the organism to attach to a variety of surfaces in an underwater environment.[1] These proteins serve to support and bind components of the adhesive holdfast composed of byssal threads.[2,3] The ability of *M. edulis* to form a tenacious adhesive bond rapidly at a solid−liquid interface entails more than just depositing these proteins on the surface. Before adhering to a surface, the mussel foot first explores and then scrubs the prospective surface by cavitation. Phenolic proteins and collagen are then injected into the already cavitated mussel foot by phenol and collagen glands, forming the plaque that is attached to the surface.[4]

Despite the complexities involved, attempts to fabricate a biomimetic version of the mussel adhesive proteins (MAP) adhesive are underway. MAP has seen recent interest in the biomedical community as a tissue adhesive. MAP has been studied for its ability to fix chondrocyte allografts internally.[5,6] The protein has also been used in experimental epikeroplasty in laboratory animals, and as an adhesive agent to increase cellular attachment to substrata.[7,8] Recent studies have also indicated that MAP enhances the attachment of osteoblasts and epiphyseal cartilage cells to substrata.[9] However, commercial uses for MAP have been limited due to the lack of understanding of how these proteins function as an adhesive. The practical application of MAP as a biocompatible adhesive has not yet been realized, as the actual anchoring mechanism is poorly understood. Despite MAPs tenacious adhesive action in the natural environment, this function has not been duplicated with the purified proteins.

The byssal threads of *M. edulis* are comprised of a collagenous matrix that is bound with a series of phenolic proteins. There have been four proteins identified in the byssal threads that are thought to serve these structural and adhesive functions: *M. edulis* foot proteins (MeFP), 1, 2, 3, and 4, collectively termed mussel adhesive proteins (MAP). It has been suggested that MeFP-1 serves as one of the initial adhesive components as well as a protective varnish on the surface of the byssal thread.[10,11] MeFP-1 is a 130 kDa protein consisting of highly conserved tandemly repeated decapeptide sequences.[12] MeFP-1 has extensive hydroxylation of tyrosine to 3,4-dihydroxyphenyl-L-alanine (L-DOPA) and of proline to hydroxyproline.[12,13] This protein is one of the first proteins described to contain

* Author to whom correspondence should be sent Center For Biofilm Engineering, 366 EPS Building, P.O. Box 173980, MSU, Bozeman, MT 59717.
† Center for Biofilm Engineering, MSU.
‡ Department of Chemical Engineering, MSU.
§ Department of Microbiology, MSU.
∥ Department of Biomedical Engineering, Case Western Reserve University.
⊥ Physical Electronics Inc.
⊗ Abstract published in *Advance ACS Abstracts*, October 1, 1997.

(1) Waite, J. H. *Int. J. Biol. Macromol.* **1990**, *12*, 139−144.
(2) Young, G. A.; Crisp, D. J. In *Adhesion 6*; Allen, K. W., Ed.; Applied Science Publishers: Oxford, U.K., 1982; p 19.
(3) Waite, J. H. *J. Biol. Chem.* **1983**, *258*, 2911−2915.
(4) Waite, J. H. *Int. J. Adhes. Adhes.* **1987**, *7*, 9−14.
(5) Pitman, M. I.; Menche, D.; Song, E. K.; Ben-Yishay, A.; Gilbert, D.; Grande, D. A. *Bull. Hosp. J. Dis. Orthopedic Institute* **1989**, *49* (2), 213−220.
(6) Grande, D. A.; Pitman, M. I. *Bulletin of the Hospital for Joint Diseases Orthop. Inst.* **1988**, *48* (2), 140−148.
(7) Robin, J. B.; Picciano, P.; Kusleika, R. S.; Salazar, J.; Benedict, C. *Arch. Ophthalmol.* **1988**, *106* (7), 973−977.
(8) Olivieri, M. P.; Rittle, K. H.; Tweden, K. S.; Loomis, R. E. *Biomaterials* **1992**, *13* (4), 201−208.
(9) Fulkerson, J. P.; Norton, L. A.; Gronowicz, G.; Picciano, P.; Massicotte, J. M.; Nissen, C. W. *J. Orthop; Res.* **1990**, *8* (6), 793−798.
(10) Waite, J. H. *Biol. Rev.* **1983**, *58*, 209.
(11) Benedict, C. V.; Waite, J. H. *J. Morphol.* **1986**, *189*, 171−181.
(12) Waite, J. H.; Housley, T. J.; Tanzer, M. L. *Biochemistry* **1985**, *24*, 5010−5014.

S0743-7463(96)01072-4 CCC: $14.00

DOPA in its primary sequence and is one of the few proteins found in nature that contains hydroxyprolines in noncollagenous sequences.[14] The β-turn structure, imparted by the hydroxyprolines, contributes a slight circular dichroism to the protein. MeFP-1 has no other secondary structure.[15]

It is believed that MeFP-2 serves a structural function, binding the collagen fibers within the byssal threads. MeFP-2 is a 42−47 kDa protein consisting of at least three repeating motifs.[16] In contrast to MeFP-1, MeFP-2 contains 6−7 mol % of the disulfide containing amino acid cystine, indicating considerable secondary structure. A similar foot protein, MgFP-2, from the closely related mussel *Mytilus galloprovincialis* has been shown to harbor internal repeats that display a high degree of homology with epidermal growth factors.[17] MeFP-3 is thought to play a role as an initial surface primer, and the function of MeFP-4 is still uncertain.

Although the biochemistry of the adhesive plaque has been extensively and elegantly characterized, relatively little work has been done to characterize the molecular interactions between components and surfaces.[18,19] A greater understanding of how MAP binds to surfaces is essential in developing MAP as a useful adhesive. To effectively understand the complex series of interactions that occurs with these proteins, it is necessary to characterize the role that each plays in the development of the adhesive bond. For this study, two components of MAP have been selected in an effort to define the protein−surface and protein−protein interactions that mediate the adhesive interactions. Once these interactions are defined, the other components of the natural adhesive can be investigated in light of these results.

The goal of this study was to investigate the adsorption of MeFP-1 and MeFP-2 (MAP_{1-2}) to polystyrene (PS) and poly(octadecyl methacrylate) (POMA) surfaces in the hydrated state using cold probe techniques in variable angle X-ray photoelectron spectroscopy (XPS) and atomic force microscopy (AFM) using fluid Tapping Mode. The adsorption of MAP_{1-2} is interpreted in light of the known surface chemistry of PS and POMA and the known biochemistry of MAP_{1-2}. Surfaces were also dehydrated at room temperature and analyzed using variable angle XPS to assess the contribution that hydration has on the adsorbed protein layer. XPS was used to quantify the elemental composition with depth of the adsorbed protein, and AFM was used to provide information about the architecture of the adsorbed protein film on the polymer surfaces.

Materials and Methods

Adsorbates, Solvents, and Substrates. MAP_{1-2} used in this study consists of two of the *M. edulis* foot proteins, (MeFP-1 and -2). Purified MAP_{1-2} from *M. edulis* was obtained from Swedish Bioscience Laboratory (Floda, Sweden) and stored desiccated at −40 °C. The amino acid composition according to the supplier is (per 1000 residues) as follows: 83 Asp, 74 Thr, 97 Ser, 64 Glu, 69 Pro, 132 Gly, 68 Ala, 50 Val, 25 Ile, 29 Leu, 30 Tyr, 12 Phe, 27 His, 115 Lys, 41 Arg, 41 Hyp, and 70 3,4-dihydroxy-L-phenylalanine (DOPA). Acetic acid−urea polyacrylamide gel electrophoresis (PAGE) indicated that the preparation consisted of approximately 80% of the two DOPA-containing proteins: MeFP-1 and MeFP-2 in equal quantities.[19] The rest of the mixture (20%) is comprised of lower molecular weight collagenic material. The protocol for the PAGE was performed using previously described methods, and the identification of MeFP-1 (130 kDa) and MeFP-2 (45 kDa) was made according to previously published results.[20]

Pure polystyrene (PS) (Aldrich Secondary Standard) and poly(octadecyl methacrylate) (POMA) (Aldrich) were dissolved in toluene for spin casting. PS was prepared as a 1.5% w/v solution in toluene. POMA was prepared as a 1.5% v/v solution in toluene. Bulk PS substrata were obtained from Plaskolite Inc. (Columbus, OH). All solvents, methanol, hexanes, and toluene (Aldrich), were obtained as HPLC grade.

Preparation of Polymer Surfaces. PS and POMA polymer films were spin cast onto 1 cm × 1 cm PS fragments for all XPS and AFM studies. PS substrata were cleaned prior to spin casting by a solvent rinse, for 5 min each, in methanol and hexanes.[21] Clean PS substrata were completely covered with 2.0 mL of polymer solution and then immediately were spin cast at 3500 rpm for 2 min. The polymer films were dried at room temperature for 24 h.

The underlying PS substrata contained trace constituents (<1% Zn, <2% Si, and <2% O) that distinguished it from the pure, spin cast PS and POMA obtained from Aldrich. These trace contaminants were used as indicators to determine purity and homogeneity of the spin cast polymer films. XPS and time-of-flight secondary ion mass spectrometry of the spin cast polymer films indicated that the films were continuous (i.e., no contaminants from the underlying polymer substratum were detected through the spin cast films). Given the limitations of variable angle XPS, an exact film thickness is difficult to determine. However, it is possible to calculate an estimated film thickness by calculating the inelastic mean free path and subsequently the escape depth of the photoelectrons. For both the PS and POMA surfaces the Zn, Si, and O impurities in the underlying PS substrata were used to gauge film thickness. The estimated film thickness of these spin cast films is approximately 10−20 nm.

Protein Adsorption Protocol. All protein films were deposited onto freshly prepared polymer surfaces that had undergone a 24 h drying period. A stock solution of 1 mg/mL of MAP_{1-2} was prepared in dilute HCl (pH 2.9) with deionized, double-distilled water, deaerated with N_2. The stock solution was maintained at pH 2.9 to prevent catechol oxidation to quinone that occurs above pH 8.5. The stock solution was stored at 5 °C. The polymer-coated substrata were placed in glass cells with entrance- and exit-tubing ports to allow for protein adsorption and subsequent rinse without exposure to the air. All glassware used was cleaned with "piranha" solution, consisting of a 70:30 mix of concentrated H_2SO_4 and 30% H_2O_2, respectively. [WARNING: Piranha solution reacts violently, even explosively with organic materials.][22]

For the XPS studies, a 50 μL aliquot of the stock solution was delivered into the glass cell containing the substratum, followed immediately by a 0.95 mL aliquot of a pH 9.2 solution (Millipore water adjusted with NaOH). The final concentration of protein was 50 μg/mL at pH 8.5. At this pH quinone formation from catechols is favored. After 1 h, the substratum was rinsed of any residual protein by flowing an aqueous solution at pH 8.5 (Millipore water adjusted with NaOH) through the reaction chamber at a rate of 100 mL/min for 1.5 min.

For the hydrated AFM studies, a much lower protein concentration was used to ensure submonolayer coverage on the substratum, so that the spatial distribution of the nucleation events could be resolved. For these experiments a 2 μL aliquot of the 1 mg/mL stock MAP_{1-2} solution was diluted in ≈1.0 mL of deionized double-distilled water at pH 2.9 to make a solution

(13) Waite, J. H.; Tanzer, M. L. *Biochem. Biophys. Res. Commun.* **1980**, *96* (4), 1554−1561.
(14) Taylor, S. W.; Ross, M. M.; Shabanowitz, J.; Hunt, D. F.; Waite, J. H. *J. Am. Chem. Soc.* **1994**, *116*, 10803−10804.
(15) Williams, T.; Marumo, K.; Waite, J. H.; Henkens, R. W. *Arch. Biochem. Biophys.* **1989**, *269*, 415.
(16) Rzepecki, L. M.; Hansen, K. M.; Waite, J. H. *Biol. Bull.* **1992**, *183*, 123−137.
(17) Inoue, K.; Takeuchi, Y.; Miki, D.; Odo, S. *J. Biol. Chem.* **1995**, *270* (12), 6698−6701.
(18) Baty, A. M.; Suci, P. A.; Tyler, B. J.; Geesey, G. G. *J. Coll. Int. Sci.* **1996**, *177*, 307−315.
(19) Suci, P. A.; Geesey, G. G. *J. Colloid Interface Sci.* **1995**, *172*, 347−457.
(20) Waite, J. H, and C. V Benedict *Methods in Enzymology* **1984**, 107, 397−413.
(21) Vargo, T. G.; Thompson, P. M.; Gerenser, L. G.; Valentini, R. F.; Aebischer, P.; Hook, D. J.; Gardella, J. A. *Langmuir* **1992**, *8*, 131.
(22) Dobbs, D. A.; Bergman, R. G.; Theopold, K. H. *Chem. Eng. News* **1990**, *68* (17), 2.

that was 2 μg/mL of MAP_{1-2}. A 25 μL aliquot of this solution was then delivered into the flow cell along with ≈1.0 mL of a dilute NaOH solution at pH 9.2, bringing the concentration of MAP_{1-2} to 25 ng/mL and the pH to 8.5. After 1 h, the substratum was rinsed of any residual protein by flowing an aqueous solution at pH 8.5 (Millipore water adjusted with NaOH) through the reaction chamber at a rate of 100 mL/min for 1.5 min.

Surface Characterization

Angle-Resolved X-ray Photoelectron Spectroscopy. Since protein adhesion to surfaces occurs in an aqueous environment, any reliable chemical analysis of the structure of the adsorbed proteins must be performed in the hydrated state. Therefore, cryostage sample-handling techniques must be employed during the analysis of a hydrated surface in ultrahigh vacuum in an effort to preserve the adsorbed species in their hydrated state. A hydrated surface can be frozen at liquid nitrogen (LN_2) temperatures and loaded onto a cold stage where the sample can be kept at LN_2 temperatures during analysis.[23,24] The structure of the adsorbed molecules at the surface are preserved at LN_2 temperature.

XPS spectra were obtained with a Physical Electronics instrument Model 5600 spectrometer (Physical Electronics, Eden Prairie, MN). A 5 eV flood gun was used to offset charge accumulation on the samples. An 800 μm diameter area was analyzed using a monochromatized Al Kα X-ray source at 350 W and a pass energy of 11.750 eV. For cold probe analysis, wet surfaces were removed from the glass cell after protein adsorption, rinsed, and mounted in the sample introduction chamber. The chamber was quickly purged with nitrogen, and the sample was immediately brought into contact with a liquid nitrogen cold finger before the sample could dehydrate. The sample remained in contact with the cold finger for 30 min, followed by immediate sample transfer to the cold stage in the analytical chamber. Most of the ice that formed on the surface when the sample was frozen quickly sublimed in the high-vacuum environment of the introduction chamber, leaving residual frozen water around the adsorbed protein molecules. The cold stage was maintained at −120 °C during analysis. Samples that were dehydrated at room temperature were removed from the final rinse and dried under an atmosphere of pure, dry N_2 in the sample introduction chamber of the XPS. Before the variable angle study was conducted, an initial 80° (near normal) high-resolution spectrum was collected. Depth profiles were performed using variable angle XPS data collected at take-off angles of 15°, 22°, 35°, and 80° from the surface. The elemental compositions at the initial 80° survey were compared with the final 80° angle study to ensure no X-ray damage of the surface had occurred during analysis. An abundance of carbon, nitrogen, and oxygen was calculated from high-resolution C_{1s}, N_{1s}, and O_{1s} peak areas by fitting the data with Gaussian functions. The binding energy scale was referenced by setting the CH_x peak maximum in the C_{1s} spectrum to 285.0 eV.[25]

The relative atomic concentrations at the different take-off angles were used with the calculated escape depths of the photoelectrons for each angle to gain insight on the elemental depth distribution of the proteins adsorbed to the polymer surfaces. The escape depths were calculated using parameters for organic compounds to calculate the inelastic mean free paths and subsequently the escape depths using equations previously defined.[26]

Atomic Force Microscopy Imaging. In order to image hydrated biological molecules on a surface using AFM, a mode of operation called fluid Tapping Mode was used. In fluid Tapping Mode the AFM cantilever is oscillated vertically at a set high frequency during $x-y$ raster scanning.[27] As the probe tip contacts the surface, its oscillations are dampened. Since the tip only intermittently "taps" the surface, this mode of operation is characterized by overall weak tip−sample interactions. This allows minimal disturbance of the adsorbed molecules during imaging.

All surfaces were imaged using a Bioscope AFM (Digital Instruments, Inc., Santa Barbara, CA). The instrument was used in fluid Tapping Mode using thin-legged, triangular, microfabricated silicon nitride cantilevers which were 100 μm in length, with nominal spring constants of 0.38 N/m and integrated pyramidal tips. The samples were attached to the fluid cell using a cyanoacrylate adhesive and dried in a laminar flow hood. The images were recorded as 1 μm × 1 μm and 2 μm × 2 μm scan areas with 512 × 512 data points/scan area. Images were recorded at scan rates of 0.8−6.1 μm/s. Scan rates were optimized to minimize hysteresis between the forward and return traces of the probe. All images were stable with time and reproducible. For analysis, images were low-pass filtered, flattened to remove sample tilt, and planefit to remove sample bow arising from hysteresis in the piezocrystal.

Results

Atomic Force Microscopy Imaging. MAP_{1-2} adsorbed to clean PS and POMA from solutions with bulk protein concentrations of 25 ng/mL were imaged in fluid Tapping Mode using AFM. Figures 1a and 1b show AFM 3-D surface images of 1 μm × 1 μm areas of the PS and POMA substrata before MAP_{1-2} adsorption. Before MAP_{1-2} adsorption, the PS and POMA surfaces are extremely smooth with few surface features and root-mean-square (rms) surface roughness values of 0.52 ± 0.13 nm and 1.06 ± 0.08 nm, respectively. Figure 2 shows AFM 3-D surface images of 1 μm × 1 μm areas of PS and POMA substrata after MAP_{1-2} adsorption. Adsorption of MAP_{1-2} to the PS surface resulted in the formation of closely packed, repeating structures as shown in Figure 2a. Cross-sectional analysis of these features revealed a near monolayer structure, making it difficult to differentiate between adjoining protein structures. The heights of these features are less than 1 nm. MAP_{1-2} adsorbed to the POMA surface displays very different protein features that appear to be linearly ordered as revealed in the 1 μm × 1 μm scan area in Figure 2b. An additional scan performed at a right angle to the first showed these features to rotate 90°, indicating that the linear features observed were not an artifact of the AFM probe tip rastering across the surface. Cross-sectional analysis reveals that these features have an average height of 5.0 ± 0.7 nm with lateral dimensions of 67 ± 17 nm (minor axis) and 177 ± 26 nm (major axis).

The 2 μm × 2 μm scan area of MAP adsorbed to PS, shown in Figure 3a, reveals that the features observed at high magnification cover larger areas of the surface, suggesting that the surfaces are homogeneous and have continuous protein coverage. The 2 μm × 2 μm scan area of MAP_{1-2} adsorbed to POMA, shown in Figure 3b, shows that the protein features on POMA are also very homo-

(23) Ratner, B. D.; Weathersby, P. K.; Hoffman, A. S.; Kelly, M. A.; Sharpen, L. H. *J. Appl. Poly. Sci.* **1978**, *22*, 643−664.
(24) Ratner, B. D.; Castner, D. G. *Colloids Surf., B* **1994**, *2*, 343−345.
(25) Ratner, B. D.; Castner, D. G. In *Surface Analysis-Techniques and Applications*; Vickerman, J. C., Reed, N. M., Eds.; John Wiley & Sons: Chichester, U.K. 1994; p 163.
(26) Seah, M. P.; Dench, W. A. *Surf. Interface Anal.* **1979**, *1*, 2−11.
(27) Drake, B.; Prater, C. B.; Weisenhorn, A. L.; Gould, S. A. C.; Albrecht, T. R.; Quate, C. F.; Cannell, D. S.; Hansma, H. G.; Hansma, P. K. *Science* **1989**, *243* (4898), 1586−1589.

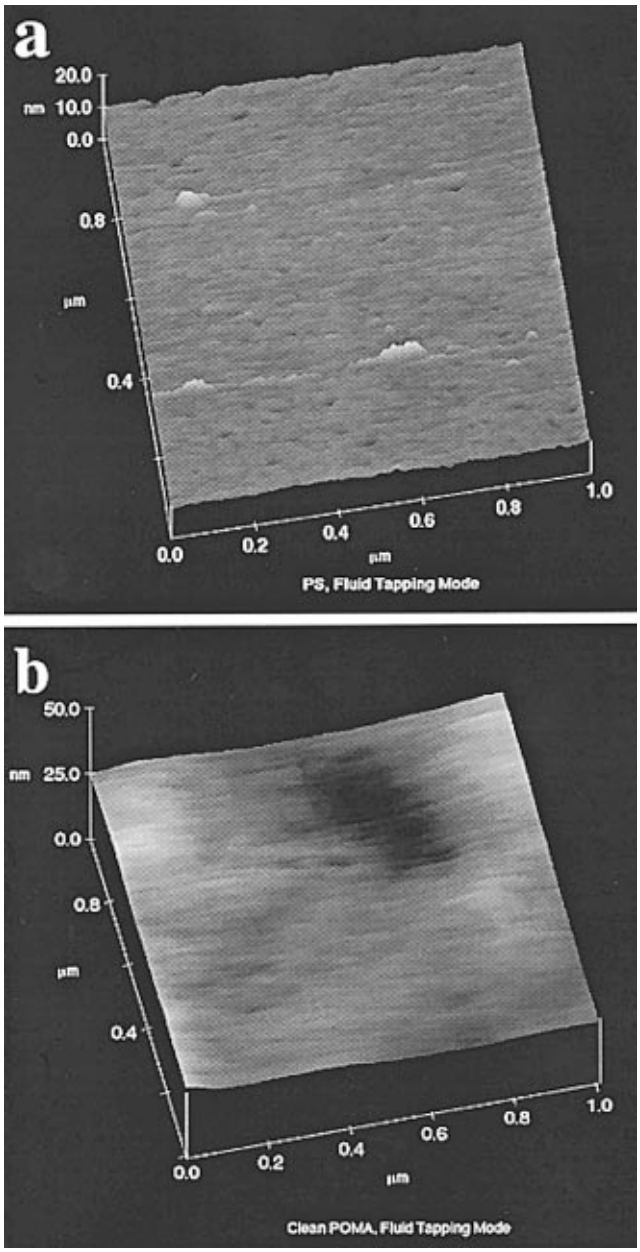

Figure 1. Fluid Tapping Mode AFM surface images of 1 μm $\times$ 1 μm area of PS (a) and POMA (b) before protein adsorption.

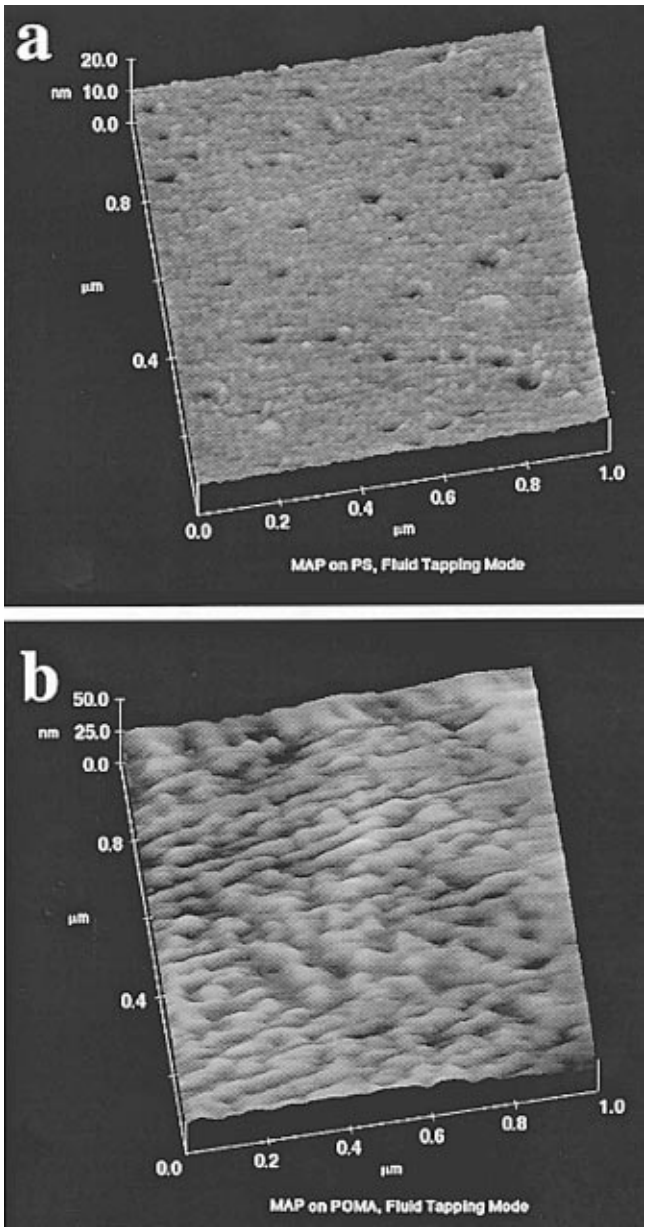

Figure 2. Fluid Tapping Mode AFM surface images of 1 μm $\times$ 1 μm area of MAP_{1-2} adsorbed to PS (a) and POMA (b).

geneous. However, there appears to be larger protein domains covering the surface, which might suggest extensive aggregation of the adsorbed protein. These features extend 6.2 $\pm$ 1.7 nm in height with lateral dimensions of 173 $\pm$ 35 nm (minor axis), with major axis values extending up to 760 nm.

Angle-Resolved X-ray Photoelectron Spectroscopy. Angle dependent XPS, performed at room temperature and LN_2 temperature, of the surfaces studied in Figures 1, 2, and 3 reveals further differences in MAP_{1-2} adsorption to PS and POMA surfaces. A detailed examination of the C_{1s} region of clean PS and POMA at a 30° take-off angle and at LN_2 temperature is shown in Figure 4. MAP_{1-2} adsorbed to PS at take-off angles of 80° and 22° at LN_2 temperature and at 22° at room temperature are given in Figure 5. MAP_{1-2} adsorbed to POMA at a takeoff angle of 80° and 22° at LN_2 temperature and at 22° at room temperature are given in Figure 6. Each peak component under these C_{1s} regions represents different carbon bonds. The C_{1s} component at a binding energy of 291.0−291.6 eV is attributed to the $\pi-\pi^*$ transition in the aromatic rings of the polystyrene. There is no detectable $\pi-\pi^*$ C_{1s} component of MAP_{1-2}. Even though these proteins have considerable aromatic character, their pi-electron systems are not dense enough to form an observable peak. The C_{1s} component at 288.0−288.8 eV arises from the N−C═O and O−C═O functionalities on the protein and the methacrylate chain, respectively. The C_{1s} component at a binding energy of 286.2−287.0 eV is attributed to the C−N and C−O functionalities in the protein and the C−O−C functionality of the POMA. The dominant C_{1s} component in both sets of spectra is at 285.0 eV. This peak originates from the aliphatic carbon in both the polymers and the protein.

The C_{1s} region of MAP_{1-2} adsorbed to PS, at LN_2 temperature at a take-off angle of 80° (Figure 5a), reveals a decrease in the aliphatic component at 285.0 eV and an increase in the 286.2 and 288.2 eV C_{1s} components when compared to clean PS (Figure 4a). This indicates MAP_{1-2} contribution to the C_{1s} region. At a take-off angle of 22° at LN_2 temperature (Figure 5b), there is a shift in the C_{1s} component at 286.2 eV toward 286.8 when compared to the spectrum collected at 80°. This peak shift suggests

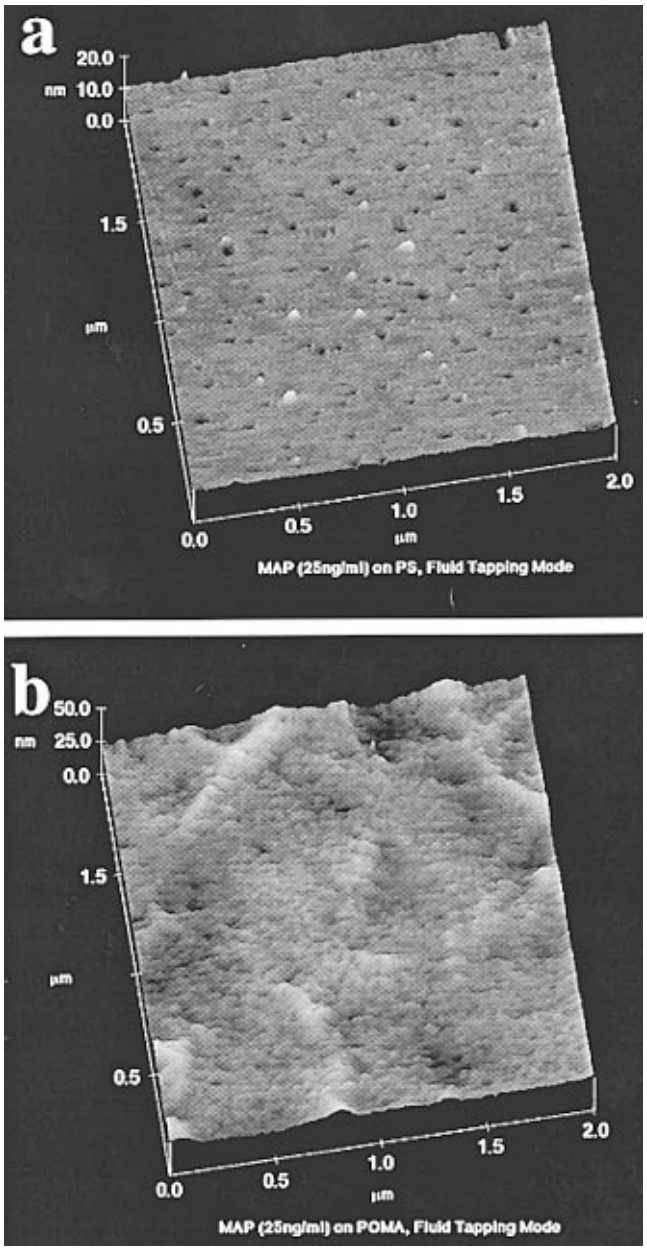

Figure 3. Fluid Tapping Mode AFM surface images of 2 μm × 2 μm area of MAP_{1-2} adsorbed to PS (a) and POMA (b).

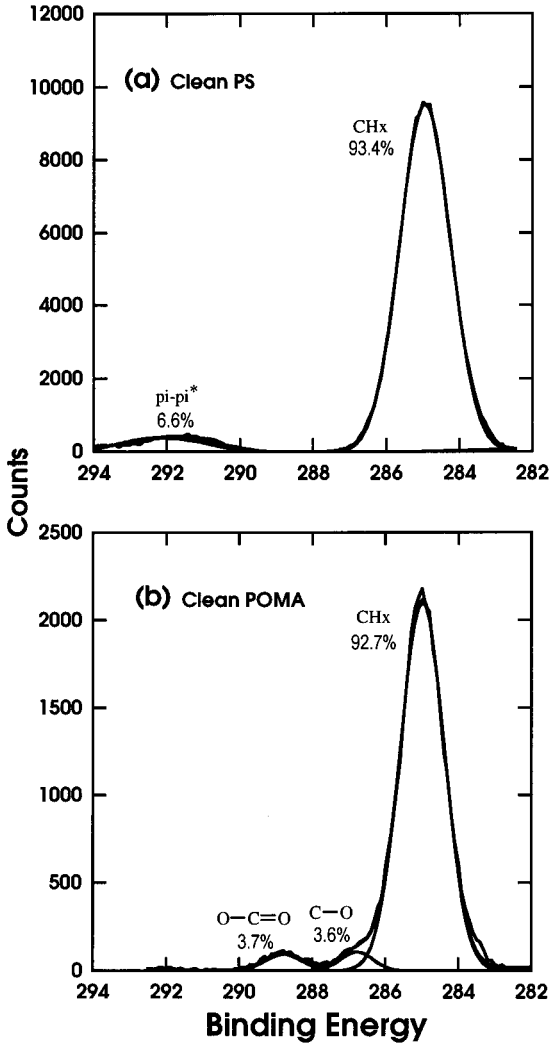

Figure 4. C_{1s} XPS spectra of clean PS (a) and POMA (b) at take-off angles of 30° at LN_2 temperature.

an increase in the signal from the C−O functionalities, as opposed to the C−N functionalities, that are present on the protein. There is more sample charging at the lower take-off angles on the surfaces analyzed at LN_2 temperature. This can be seen in the broader peak components in both sets of spectra obtained at LN_2. However, charging does not account for the peak shift observed between 286.2 and 286.8 eV since not all of the peak components are shifted. There is also an increase in the intensity of the 286.8 and 288.2 eV C_{1s} components, as compared to the spectrum at 80°, indicating that at the angle approaching glancing, the signal from the PS is decreasing while that of the adsorbed protein is increasing. The C_{1s} region of MAP_{1-2} adsorbed to PS and dehydrated at room temperature (Figure 5c) shows an increase in the 291.6 eV C_{1s} component that is attributed to the $\pi-\pi^*$ transition of the aromatic rings of the PS. There is also a decrease in the peak area of the 286.8 and 288.1 eV components from the adsorbed protein, as compared to the surfaces analyzed at LN_2 temperature. This indicates that PS is contributing to the spectra more when the surface is analyzed after dehydration at room temperature than when the surface is analyzed at LN_2 temperature. Furthermore, a peak at 289.0 eV (acid or ester functionality) appears in the spectra upon dehydration. This functionality is not part of the MAP_{1-2} or the underlying PS substrata. It is unclear whether this species is present in the MAP_{1-2} mixture and migrated to the surfaces upon dehydration or adsorbed to the surface during dehydration.

The C_{1s} region of MAP_{1-2} adsorbed to POMA, at LN_2 temperature at a take-off angle of 80° (Figure 6a), reveals a shift in the C_{1s} component at 286.7 and 288.8 eV (clean POMA) toward 286.1 and 288.3 eV, respectively. This is a result of an increase in the signal from the C−N functionalities that are present from the adsorbed protein. There is also a decrease in the aliphatic component at 285.0 eV and an increase in the 286.1 and 288.3 eV C_{1s} components when compared to those of clean POMA (Figure 4b). This also indicates MAP_{1-2} contribution to the C_{1s} region. At a take-off angle of 22° at LN_2 temperature (Figure 6b), there is a shift in the 286.1 and 288.3 eV components back to 286.7 and 288.8 eV, respectively. This could be a result of an increase in the signal from the C−O functionalities that are present from the adsorbed protein. However, there is no significant increase in the area of the peaks which are attributed to the protein. The fact that the AFM images show homogeneous coverage and there is no significant difference in these peak areas at the two different take-off angles suggest that the adsorbed protein layer on the POMA is much less densely packed than on the PS surface, where

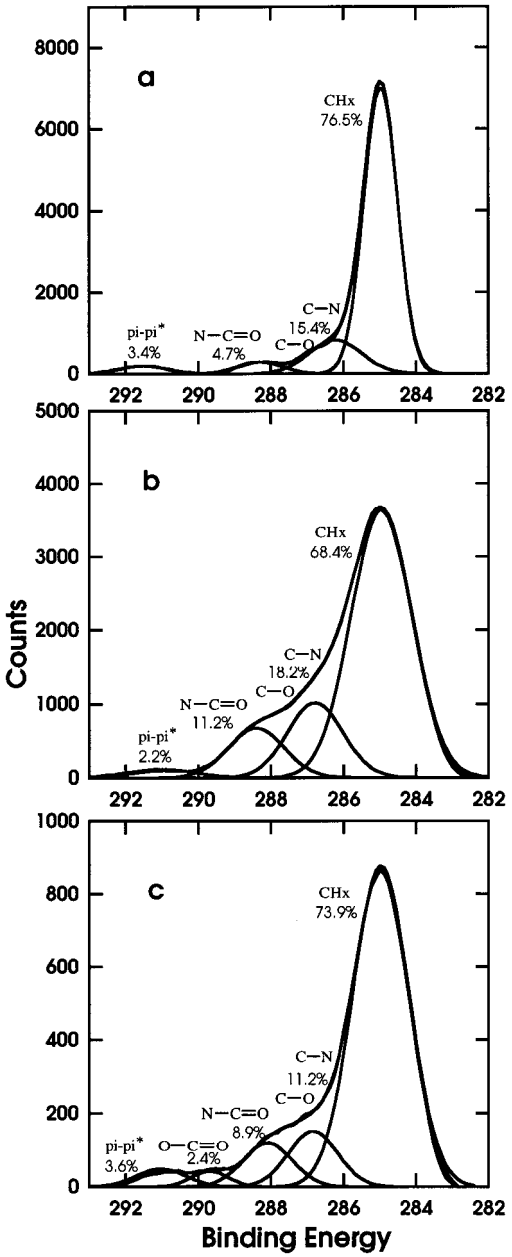

Figure 5. C_{1s} XPS spectra of MAP_{1-2} adsorbed to PS at 80° (a) and 22° (b) takeoff angles at LN_2 temperature and at 22° take-off angles (c) at room temperature.

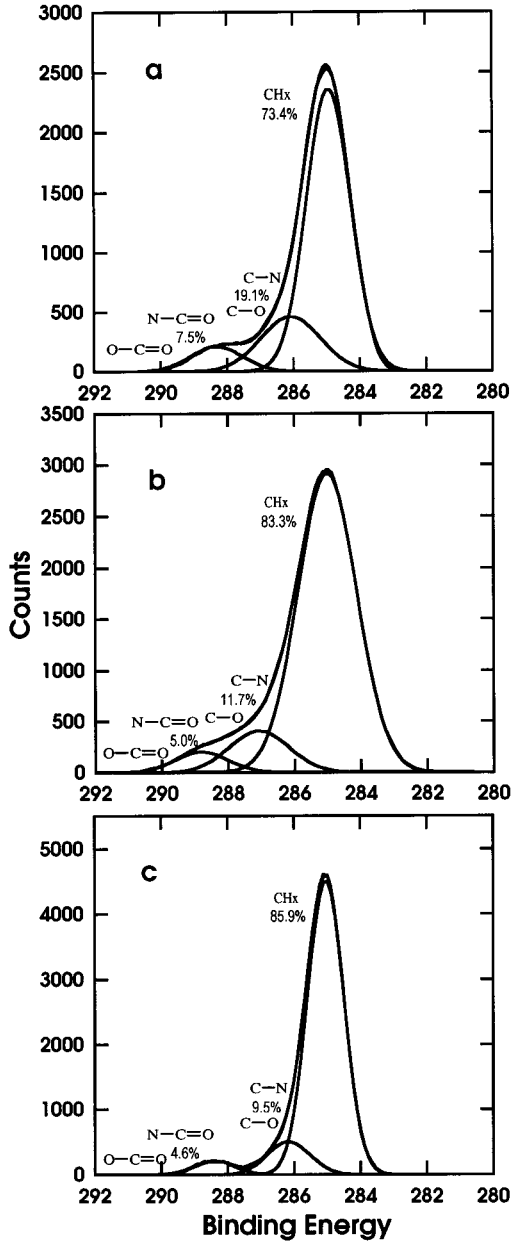

Figure 6. C_{1s} XPS spectra of MAP_{1-2} adsorbed to POMA at 80° (a) and 22° (b) take-off angles at LN_2 temperature and at 22° take-off angles (c) at room temperature.

the signal intensity at the 22° take-off angle (LN_2) appears to be contributed primarily by MAP_{1-2}. However, these data are difficult to interpret due to the insufficient knowledge, to date, concerning the analyses of biological surfaces at LN_2 temperature using XPS. The C_{1s} region of MAP adsorbed to POMA and dehydrated at room temperature (Figure 6c) shows a decrease in the 286.5 and 288.5 eV components and is approaching a pure POMA spectrum. This indicates that more of the POMA is contributing to the spectra when the surface is dehydrated at room temperature than when it is at LN_2 temperature during analysis. It was also observed that at LN_2 temperature the high-resolution C_{1s} peak components were broader than the same spectra taken at room temperature. This might be attributed to less efficient charge compensation at LN_2 temperatures at the lower take-off angles. How this would affect signal intensity is currently unknown.

Figure 7 shows a plot of the atomic concentration of MAP_{1-2} adsorbed to PS (Figure 7a) and POMA (Figure 7b) at take-off angles of 80°, 35°, 22°, and 15°, corresponding to sampling depths of 84.3, 49.1, 32.1, and 22.2 Å, respectively. The atomic concentrations when analyses were performed at LN_2 temperature and when the samples were dehydrated at room temperature are shown. At all depths, on both PS and POMA exposed to MAP_{1-2}, the atomic concentration of nitrogen and oxygen was lower when the samples were dehydrated and analyzed at room temperature as compared to the surfaces analyzed at LN_2 temperature. This suggests that more of the substratum is contributing to the spectra upon dehydration of the adsorbed MAP_{1-2}, which decreases the relative signal intensity of the adsorbed MAP_{1-2}. When MAP_{1-2} adsorbed to PS was analyzed at LN_2 temperature and room temperature, the surface dehydrated at room temperature experienced an average 2.6% loss in nitrogen and a 1.9% loss in oxygen. Furthermore, the atomic concentrations for MAP_{1-2} adsorbed to PS, when analyzed at LN_2 and room temperature after dehydration converge at the 80° take-off angle. This indicates that the same amount of protein is being sampled on the surface at the 80° take-off

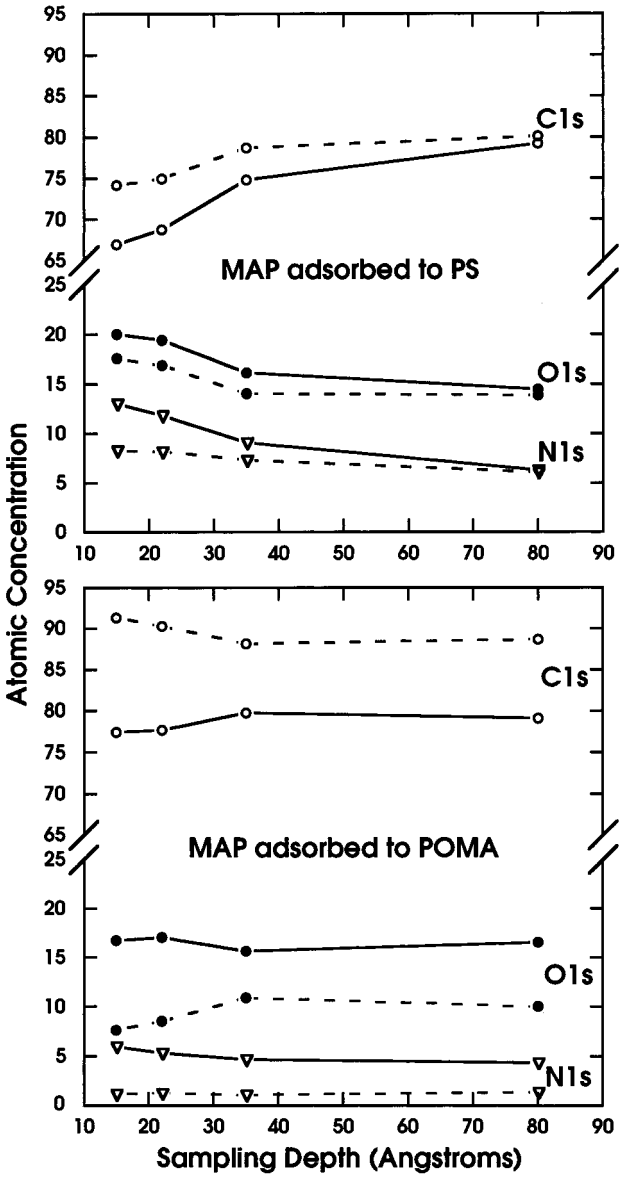

Figure 7. Summary of angle-resolved XPS data of MAP_{1-2} adsorbed to PS (top) and POMA (bottom) at LN_2 temperature (solid line) and room temperature (broken line).

angle regardless of whether water is present. In contrast, when MAP_{1-2} adsorbed to POMA was analyzed at LN_2 temperature and at room temperature after dehydration, the surface experienced a loss of nitrogen and oxygen upon dehydration of 3.9% and 7.2%, respectively. Furthermore, the atomic concentrations for the LN_2 and room temperature studies do not converge at the 80° take-off angle for MAP_{1-2} adsorbed to POMA. This suggests that upon the removal of water the protein architecture is more perturbed on the POMA surface than on the PS surface.

Discussion

The study of the adsorption behavior of proteins has primarily been focused on globular proteins. Theories concerning the adsorption process of globular proteins have stressed the importance of structural rearrangements, electrostatic interactions, and the displacement of interfacial water as the processes of primary importance.[28−30] However, specific functional group chemistry is not generally discussed as a contributing factor in adsorption. The results presented here indicate that the adsorption behavior of MAP_{1-2} is influenced by both functional group chemistry and the displacement of ordered water from the interface. The relative contribution of these two factors depends upon the surface chemical properties of the substratum. The data indicate that protein−surface as well as protein−protein interactions, with specific functional groups on MAP_{1-2}, play significant roles in driving adsorption to polymer surfaces that display different chemical properties. This is consistent with MAP_{1-2}'s role as a component of a multifunctional adhesive used by *M. edulis*.

The MAP_{1-2}-surface interactions that are available in the polymer−protein system studied here are constrained by the surface chemical properties of PS and POMA as well as the aqueous environment. PS provides a hydrophobic surface with an aromatic character and a medium surface free energy (88° water contact angle). Possible interactions that could occur on this surface would be a $\pi-\pi$ overlap between the DOPA residues in MAP_{1-2} and the aromatic rings of PS and cation$-\pi$ interactions between the protonated amines of the lysines and the π-face of the styrene rings. In contrast, the POMA surface provides a hydrophobic low-energy surface (104° water contact angle) with an aliphatic functionality. Interactions with specific functional groups are not likely to occur between MAP_{1-2} and a POMA surface because there are no functional groups on POMA that would mediate such interactions. Interactions involving the ester functionalities of POMA are sterically hindered by the C_{18} hydrocarbon chains and are unavailable for interactions with MAP_{1-2}, as indicated by the high water contact angle.

We have previously presented AFM images of MAP_{1-2} adsorbed to PS and POMA after dehydration at room temperature.[18] Comparison with the present images obtained under hydrated conditions reveals that the architecture of the adsorbed protein on both PS and POMA surfaces is perturbed as a result of dehydration. The instability of MAP_{1-2} adsorbed to the POMA surface, following dehydration, is reflected by the increased relief of the protein film and the lateral displacement and aggregation of the proteins on the surface, as seen in the AFM images (previously published). In contrast to the POMA surface, the stability of MAP_{1-2} adsorbed to the PS surface is not as dependent on the presence of water. Although MAP_{1-2} adsorbed to PS gains relief as a result of dehydration, it does not undergo lateral displacement or aggregation. These results suggest that the presence of water is not as important in stabilizing the interactions between MAP_{1-2} and PS as between MAP_{1-2} and POMA.

XPS data also revealed that hydration played a significant role in MAP_{1-2}−surface interactions on both PS and POMA. The increase in relief of the protein film on both surfaces is due to the collapse of the protein matrix upon removal of water by dehydration. This results in greater signal intensity from the underlying substratum for both PS and POMA. This is reflected in the reduced atomic concentration of the protein, as indicated by nitrogen and oxygen, when surfaces were dehydrated and analyzed at room temperature as compared to analysis at LN_2 temperature. The XPS evidence that dehydration resulted in a greater decrease in atomic concentration of MAP_{1-2} on POMA than on PS supports the AFM observation that POMA permitted more lateral surface displacement of MAP than PS. The reorientation of MAP_{1-2} on POMA as a result of dehydration was sufficient to cause shifts in atomic concentrations of MAP_{1-2} at all XPS take-off angles used in these studies. Dehydration-induced

(28) Haynes, C. A., Sliwinsky, E., Norde, W. *J Colloid Interface Sci.* **1994**, *164*, 394−409.
(29) Ball, R. A.; Jones, R. A. L. *Langmuir* **1995**, *11*, 3542−3548.
(30) Haynes, C. A.; Norde, W. *J. Colloid Interface Sci.* **1995**, *169*, 313−328.

shifts in atomic concentration were only observed at the shallower sampling depths on PS. The lateral displacement and reorientation on the POMA surface upon dehydration reflect the instability of the MAP_{1-2}−POMA interaction in the absence of water and reveal, again, the importance of specific functional group interactions in stabilizing protein adsorption to the PS surface.

It is hypothesized here that the aromatic residues of MAP_{1-2} are not involved in adsorption on the POMA surface, and therefore, are free to interact with other functional groups within MAP_{1-2}. There are several interactions that have been proposed to play important roles in protein−protein interactions on the basis of the chemistry of MAP_{1-2}, including hydrogen bonding, metal−ligand complexes, the formation of Michael-type addition compounds derived from *o*-quinones, and charge transfer complexes.[1] Recently, cation−π interactions have also been shown to occur with high-binding enthalpies in systems containing cations and aromatic rings.[31] In the system studied here three of these interactions could be responsible for the protein−protein interactions in MAP_{1-2}: hydrogen bonding, charge transfer interactions between the aromatic residues of MAP_{1-2}, and cation−π interactions. Charge transfer interactions are promoted at an elevated pH, above 8.5 (the pH during adsorption). At this pH the catechol functionality on the DOPA can undergo a spontaneous reverse dismutation to the *o*-quinone that is capable of interacting through a quinhydrone charge transfer complex that is stabilized by $\pi-\pi$ overlap interactions. Cation−π interactions can be considered an electrostatic interaction between the protonated amines of the lysines and the π-face of the aromatic amino acids in the protein. Michael-type additions between the protonated amines of the lysines and the quinones have not been shown to occur spontaneously with these proteins. However, there is a catechol oxidase found in the natural adhesive holdfast that catalyzes the oxidation of catachols to quinones which is believed to promote this cross-linking reaction. The possibility of this type of cross-linking occurring in the system described here is unlikely since the enzyme is not present. Thus, the charge transfer complex that is stabilized by $\pi-\pi$ overlap interactions and cation−π interactions are the most likely candidates for causing the aggregation of MAP_{1-2} on the POMA surface. Evidence for this behavior was demonstrated by AFM and is shown schematically in Figure 8.

In the case of MAP_{1-2} adsorption to POMA, water likely provides the driving force for adsorption through the displacement of interfacial water. For human blood plasma albumin and bovine pancreas ribonuclease adsorption to PS, it has been shown that in the absence of dominant enthalpic interactions between specific groups of the surface and the protein, the proteins affect the overall adsorption by dehydrating or displacing water from the surface.[32] On a surface like the POMA surface this type of interaction would be the dominant protein−surface interaction. Such adsorption increases the entropy of the system providing the driving force for adsorption. This type of protein−surface interaction results in a tenaciously bound protein layer with no specific functional group interactions between the surface and the adsorbed MAP_{1-2}, as long as the driving force provided by the surrounding aqueous environment is present. Thus, aggregation of the adsorbed protein is favored by the lack of potential interactions between the protein and the substratum.

When MAP_{1-2} is adsorbed on PS, aggregation is not observed, rather individual, tightly packed structures resembling individual protein molecules project from the surface. Since the PS surface has considerable aromatic character, the adsorbed MAP_{1-2} may interact with the aromatic rings of PS through $\pi-\pi$ overlap interactions and cation−π interactions further strengthening the interaction with the substratum and reducing the likelihood of protein−protein interactions, as shown in Figure 8. The adsorption of a series of aromatic compounds has been previously studied, and it was found that the orientation of the adsorbed aromatic domains followed several rules.[33] In the absence of chemisorbable functional groups that interfere with the aromatic framework, and in the absence of bulky electronegative constituents on the aromatic framework, the *o*-quinones were found to adsorb parallel to the surface when $\pi-\pi$ overlap interactions were involved in adsorption. Likewise, the DOPA residues in MAP_{1-2} may orient themselves parallel to the aromatic rings of PS to facilitate $\pi-\pi$ overlap interactions. The protonated amines of the lysines may also interact with the π-face of the styrene rings through cation−π interactions, and they may interact with the aromatic amino acids of MAP_{1-2} to facilitate protein−protein interactions. In the case of MAP_{1-2} adsorption to PS, water may provide the initial driving force for adsorption through the displacement of interfacial water, but binding is then reinforced through these specific functional group interactions between the proteins and the surface. It should also be noted that at the lower take-off angles at LN_2 temperature, charge buildup on these insulating surfaces may not have been sufficiently compensated. The extent to which uncompensated charge buildup on the surface and/or the presence of frozen water affects signal intensity is uncertain and remains to be determined. Furthermore, it is currently uncertain what the concentrations of Mefp-1 and Mefp-2 are on the surface. A study that has yet to be undertaken is a set of solution depletion experiments to measure the amount of protein adsorbed to the surface by measuring the residual left in the bulk. This may provide further insight into the differences between adsorption of MAP_{1-2} on these polymer surfaces.

Conclusions

The LN_2 temperature XPS analysis and hydrated AFM images demonstrate that differences in substratum chemistry will influence protein adsorption. The data support the hypothesis that interactions requiring the presence of water are more important in stabilizing MAP_{1-2} films on POMA than on PS. Interactions between specific functional groups on MAP_{1-2} and PS, possibly involving $\pi-\pi$ overlap between DOPA residues of MAP_{1-2} and the aromatic rings of PS and cation−π interactions between the protonated amines of lysine and the π-face of the styrene rings stabilize MAP_{1-2} films on this substratum during dehydration. These results offer insight into the types of molecular interactions that control surface adsorption of biological molecules in aqueous environments. This research also shows that when MAP_{1-2} is subjected to dehydration on a surface, changes in the structure of the adsorbed protein film can be detected by XPS and AFM, demonstrating the role of water in stabilizing interactions that mediate MAP_{1-2} adsorption to PS and POMA surfaces. However, the magnitude of the change depends on what types of interactions mediate protein adsorption to the surface. From the present study it appears that irreversible protein adsorption involving

(31) Dougherty, D. A. *Science* **1996**, *271*, 163−167.
(32) Norde, W., Lyklema, J. *J. Colloid Interface Sci.* **1979**, *71*, 350−366.
(33) Soriaga, M. P., Hubbard, A. T. *J. Am. Chem. Soc.* **1982**, *104*, 2735−2742.

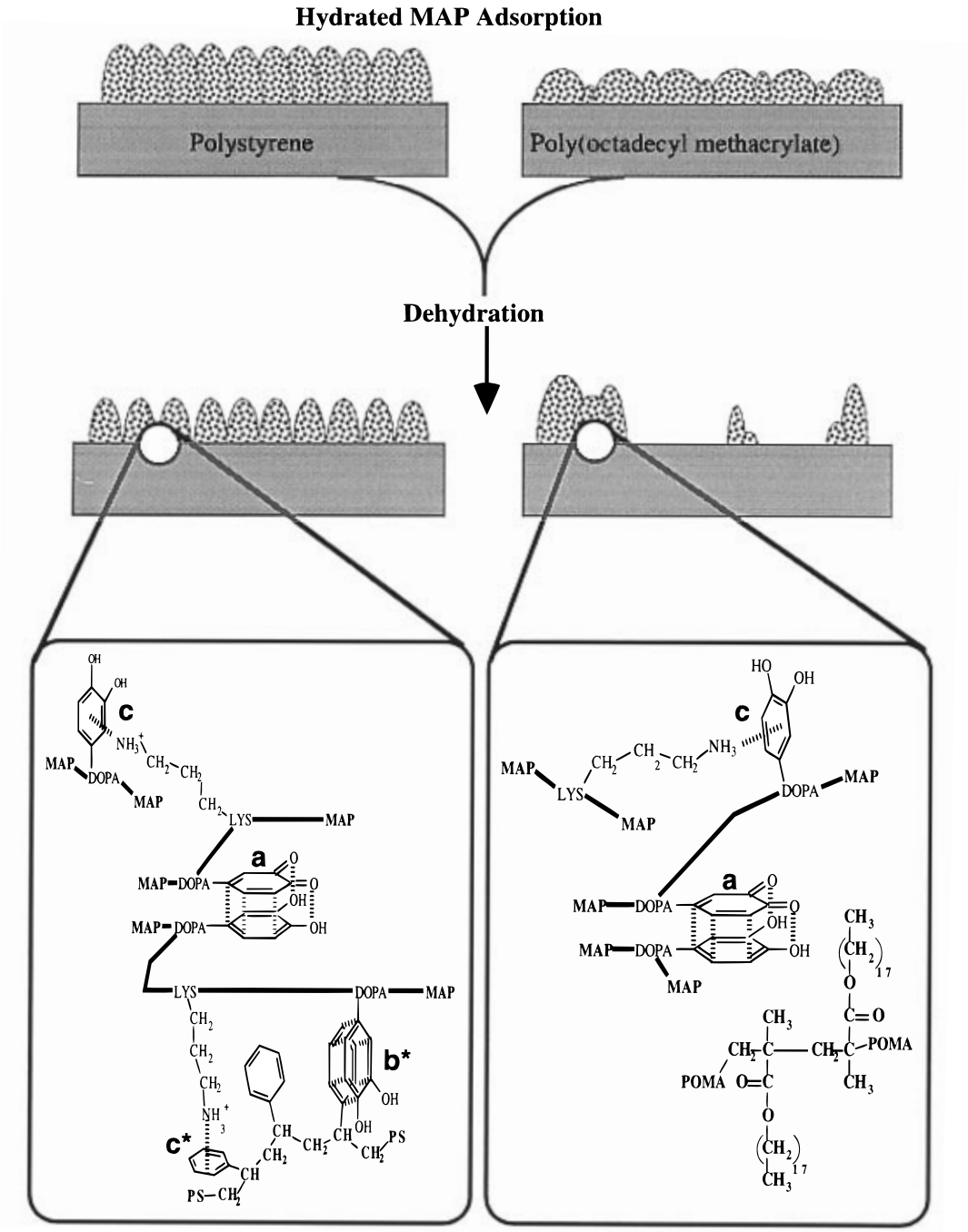

Figure 8. Schematic representation of the AFM images observed as related to the mechanisms available for adsorption: a = quinhydrone charge transfer complex, b = $\pi-\pi$ overlap interactions, c = cation$-\pi$ interactions, * = protein−surface interactions (hydorgen-bonding interactions not shown).

specific functional group interactions will experience much less disruption upon dehydration than interactions that only require the presence of water as the driving force for adsorption.

Acknowledgment. The authors gratefully acknowledge the Interfacial Chemical Analysis Lab at Montana State University for their guidance and expertise in surface analysis and the Murdock Charitable Trust for a grant to obtain the instrumentation used for this research. Also, thanks are extended to Dr. Herbert Waite at the University of Delaware for his insight into the mussel adhesive proteins. Thanks are also extended to Dr. Larry Davis at Physical Electronics Inc. in Minneapolis, MN for his generous gift of many hours of instrument time. The authors also acknowledge the Center for Cardiovascular Biomaterials at Case Western Reserve University for the use of their AFM facilities. This research was supported by the Office of Naval Research under Grant N0014-93-1-0168 and N0014-95-11086, a grant to Dr. Gill G. Geesey from 3M and the NSF under cooperative agreement EEC 8907039.

LA9610720